Effect of natural organic matter (NOM) on Cu(II) adsorption by multi-walled carbon nanotubes: Relationship with NOM properties

ARTICLE *in* THE CHEMICAL ENGINEERING JOURNAL · AUGUST 2012

Impact Factor: 4.32 · DOI: 10.1016/j.cej.2012.06.118

4 AUTHORS, INCLUDING:

Weiling Sun
Peking University
49 PUBLICATIONS **590** CITATIONS
SEE PROFILE

Si Li
National University of Singapore
4 PUBLICATIONS **54** CITATIONS
SEE PROFILE

Chemical Engineering Journal 200-202 (2012) 627–636

Contents lists available at SciVerse ScienceDirect

Chemical Engineering Journal

journal homepage: www.elsevier.com/locate/cej

Effect of natural organic matter (NOM) on Cu(II) adsorption by multi-walled carbon nanotubes: Relationship with NOM properties

Wei-Ling Sun [a,b,*], Jing Xia [a], Si Li [b], Fang Sun [a]

[a] Department of Environmental Engineering, Peking University, The Key Laboratory of Water and Sediment Sciences, Ministry of Education, Beijing 100871, China
[b] Key Laboratory for Urban Habitat Environmental Science and Technology, School of Environment and Energy, Peking University Shenzhen Graduate School, Shenzhen 518055, China

HIGHLIGHTS

- Effect of NOM characteristics on the Cu adsorption by MWCNTs was investigated.
- Cu adsorption by MWCNTs increased with increasing NOM concentration.
- The aromaticity is a key factor for NOM sorption on MWCNTs.
- O-containing functional groups play critical roles in NOM effect on Cu adsorption.

ARTICLE INFO

Article history:
Received 5 April 2012
Received in revised form 25 June 2012
Accepted 26 June 2012
Available online 2 July 2012

Keywords:
Natural organic matter
Cu(II)
Multi-walled carbon nanotubes
Adsorption

ABSTRACT

The effect of natural organic matter (NOM) on Cu(II) adsorption by multi-walled carbon nanotubes (MWCNTs) was investigated. Particular attention was paid to the relationship between NOM properties and NOM adsorption and their effects on the Cu(II) adsorption by MWCNTs. The results showed that the NOM adsorption data were well fit to the Freundlich isotherm model, and the MWCNTs that had higher oxygen content had lower K_F (Freundlich constants) values. The K_F values for the different types of NOM varied greatly and were proportional to the aromatic carbon content, the specific ultraviolet absorbance at 275 nm, and the TOC-normalized fluorescence intensity of the F3 peak at ~460 nm. In contrast, they had negative linear correlations with the absorbance ratios at 250 nm and 365 nm and the TOC-normalized fluorescence intensity of the F1 peak from 250 nm to 300 nm. The results indicated that π–π and hydrophobic interactions were the predominant NOM adsorption mechanisms by the MWCNTs. The Cu(II) adsorption by the MWCNTs increased with increasing NOM concentrations due to the complexing of Cu(II) with the adsorbed NOM. This was confirmed by XPS and FTIR spectra. The increased degree of Cu(II) adsorption was positively correlated with the carboxyl carbon content, carboxyl group content, and the polarity index of the NOM. The findings in this study highlight that the NOM characteristics are responsible for controlling the NOM adsorption and its effects on heavy metal sorption by MWCNTs.

1. Introduction

Carbon nanotubes (CNTs), which are categorized into two main species, single-walled nanotubes (SWCNTs) and multi-walled nanotubes (MWCNTs), are allotropes of carbon that possess exceptional physicochemical, optical, and mechanical properties [1,2]. They have been studied widely with regard to their potential environmental application as effective adsorbents of heavy metals [3–8] and organic chemicals [9] during solid-phase extraction and water treatment. Due to extensive applications, CNTs have inevitably been released into the environment. As a result, there are serious concerns over their health and environmental risks [10,11] with increasing evidence of the toxicity of CNTs [12]. The adsorption of toxic substances by CNTs may enhance the toxicity of CNTs and further affect the fate and transfer of toxic substances in the environment [9]. Therefore, an investigation of the adsorption behavior of CNTs is needed to evaluate the environmental and health risks of CNTs.

Natural organic matter (NOM) is a complex and heterogeneous mixture of a diverse group of molecules [13]. Humic acid (HA) and fulvic acid (FA) are its main components, accounting for, on average, 10% and 40%, respectively, of dissolved organic carbon [14]. NOM is ubiquitous in the natural environment. Manufactured CNTs will inevitably interact with NOM after they are released into the environment [15–17]. Moreover, due to the aromatic, carboxylic

* Corresponding author at: Department of Environmental Engineering, Peking University, The Key Laboratory of Water and Sediment Sciences, Ministry of Education, Beijing 100871, China. Tel./fax: +86 10 62767014.
E-mail address: wlsun@pku.edu.cn (W.-L. Sun).

1385-8947/$ - see front matter © 2012 Published by Elsevier B.V.
http://dx.doi.org/10.1016/j.cej.2012.06.118

and phenolic moieties that are found in NOM molecules, NOM can also complex with toxic substances [18–20]. Consequently, the adsorption of toxic substances by CNTs might be altered, thus affecting the fate and transport of the CNTs [7,17]. Recognizing the influence of NOM on the adsorption of pollutants by CNTs is necessary to define their fate in the environment. However, only a limited number of studies have examined the significance of NOM on the adsorption of toxic substances by CNTs.

Recent studies have shown that NOM can influence the sorption of heavy metals [7] and organic contaminants [16] by adsorbing to the surfaces of CNT particles and complexing with metals and organic contaminants. NOM varies widely according to its origin, and its composition is influenced by factors such as water chemistry, climate, and carbon source [14]. Hyung and Kim [15] found that the degree of NOM adsorption by MWCNTs varied greatly depending on the type of NOM and was closely related to the aromatic carbon content and molecular weight of the NOM. Moreover, the composition and the source of NOM could be key factors that contribute to the stabilization of nanoparticles in aquatic environments [21]. However, to date, few studies have considered how the composition of NOM contributes to the sorption of metals by CNTs. It is highly important to solve this problem with relation to MWCNTs, which are more widely used than SWCNTs.

In this paper, Cu(II) was selected as a model heavy metal ion because of its common existence in aqueous environments, and the adsorption of Cu(II) on MWCNTs was investigated in the presence of seven types of NOM. The aim of the present research was to: (1) determine the NOM adsorption by MWCNTs and analyze the interaction mechanisms between NOM and MWCNTs, (2) evaluate the influence of NOM on Cu(II) sorption by MWCNTs and investigate the relationship between NOM properties and its effect on Cu(II) adsorption, and (3) further delineate the underlying interaction mechanisms between NOM and MWCNTs and, additionally, NOM and Cu(II).

2. Materials and methods

2.1. Materials

Three types of MWCNTs with the same diameters and similar surface areas were used in this study, including pristine MWCNTs (MWCNTs-1), hydroxy (3.70 wt%) MWCNTs (MWCNTs-2), and carboxyl (2.56 wt%) MWCNTs (MWCNTs-3). The physical characteristics of the MWCNTs according to the manufacturers' data were: purity >95%, outer diameter 8–15 nm, inner diameter 3–5 nm, length ~50 μm, specific surface area > 233 m^2/g, ash < 1.5% (wt%), electrical conductivity > 100 s/cm, and tap density 0.27 g/cm^3. MWCNTs-1 is produced by acetylene catalytic decomposition over Ni-based catalyst, and often exists in bundles. MWCNTs-2 and MWCNTs-3 are produced by $KMnO_4$ oxidation in HCl solution at different temperature and $KMnO_4$ concentration. They were purchased from Chengdu Organic Chemistry Co., Chinese Academy of Sciences. Four types of HA (Leonardite standard HA (LSH), Pahikee peat reference HA (PPH), Waskish peat reference HA (WPH), and Elliott soil standard HA (ESH)), one type of FA (Nordic aquatic reference FA (NAF)), and two types of aquatic NOM (Suwannee river aquatic NOM (SRN) and Nordic reservoir aquatic NOM (NRN)) were purchased from the International Humic Substances Society (IHSS). The elemental compositions and ^{13}C NMR estimates of the carbon distributions in the IHSS samples are provided in Table 1. The NOM stock solutions were prepared by mixing a known amount of NOM with ultrapure water for 24 h. The dissolution of NOM was facilitated by adding NaOH to increase the solution pH to 7. Milli-Q water (18 MΩ cm) and analytical reagent-grade chemicals were used throughout the experiments.

2.2. Characterization of MWCNT samples

A 1.0 mg of the prepared sample was used to determine the C, H, and N contents of the MWCNTs using a CHNS/O analyzer (Elementar, Vario EL, Germany). The oxygen content was calculated by subtracting the percentage of C, H, and N from 100%.

XPS data were collected on an AXIS-Ultra instrument from Kratos Analytical (UK) using monochromatic Al Kα radiation (225 W, 15 mA, 15 kV) and low-energy electron flooding for charge compensation. To compensate for surface charge effects, the binding energies were calibrated using the C 1s hydrocarbon peak at 284.80 eV. The data were converted into VAMAS file format and imported into the CasaXPS software package for manipulation and curve fitting.

FTIR spectra were recorded with an FTIR spectrometer (Tensor27, Bruker, Germany). Approximately 1 mg of dry powdered sample was mixed gently with 100 mg KBr before pressing into a translucent sheet. The FTIR spectra were recorded from 400 to 4000 cm^{-1} at 1.0 cm^{-1} intervals in transmission mode.

Table 1
Elemental compositions and ^{13}C NMR estimates of carbon distributions for NOM samples.

Sample	Elemental compositions (%)								(O+N)/C
	H_2O	Ash	C	H	O	N	S	P	
LSH	7.2	2.58	63.81	3.7	31.27	1.23	0.76	<0.01	0.38
PPH	10.4	1.72	56.84	3.6	36.62	3.74	0.7	0.03	0.54
WPH	6.93	1.6	54.72	4.04	38.54	1.47	0.36	0.31	0.55
ESH	8.2	0.88	58.13	3.68	34.08	4.14	0.44	0.24	0.50
NAF	9.2	0.45	52.31	3.98	45.12	0.68	0.46	<0.01	0.66
SRN	8.15	7	52.47	4.19	42.69	1.1	0.65	0.02	0.63
NRN	–	41.4	53.17	5.67	40.06	1.1	–	–	0.58

Sample	Relative carbon contributions (%)					
	Carbonyl 220–190 ppm	Carboxyl 190–165 ppm	Aromatic 165–110 ppm	Acetal 110–90 ppm	Heteroaliphatic 90–60 ppm	Aliphatic 60–0 ppm
LSH	8	15	58	4	1	14
PPH[a]	2	20	37	7	10	25
WPH	8	18	42	6	8	18
ESH	6	18	50	4	6	16
NAF	10	24	31	7	12	18
SRN	8	20	23	7	15	27
NRN	8	21	19	5	16	31

[a] Determined using Solid-State-FT-NMR (AV 400 MHz WB, Bruker Biospin, Germany) in this study.

2.3. Characterization of NOM samples

The concentrations of dissolved organic carbon (DOC) in the NOM solutions were determined using a total organic carbon analyzer (TOC-V_{CPN}, Shimadzu, Japan). The relative precision of the DOC analyses was <3% as determined by repeated measurements.

The specific ultraviolet absorbance (SUVA) of each water sample at 275 nm was calculated by dividing the absorbance at 275 nm by the DOC level of the solution. The absorbance was measured using a UV–visible spectrophotometer (UV-1800, Shimadzu, Japan) with a 1 cm quartz cell. The DOC concentrations were also suitably diluted before the absorbance determinations.

Synchronous fluorescence spectra for excitation wavelengths ranging from 200 nm to 700 nm were recorded using a constant offset ($\Delta\lambda$ = 30 nm) between excitation and emission wavelengths. The NOM solutions were diluted to a final DOC concentration of 8–10 mg/L to avoid the inner filter correction [22]. The fluorescence spectra were normalized by the DOC to compare the spectroscopic characteristics.

Molecular weight distribution of NOM was determined with size exclusion chromatography (SEC), An Agilent 1200 high performance liquid chromatography coupled with a TSK-GEL G4000PW_{XL} (10 μm, 7.8 × 300 mm) (TOSOH Co., Ltd. Japan) and a diode array detector was used, and the detecting wavelength was set as 254 nm. The mobile phase was a mixture of 0.03 M NaCl, 0.001 M Na_2HPO_4, and 0.001 M NaH_2PO_4 with a flow rate of 0.5 mL/min.

2.4. Batch adsorption experiments

Batch experiments were conducted by mixing 50 mL of a 0.01 mol/L $CaCl_2$ solution with 10 mg of MWCNTs, followed by 30 min of sonication in 100 mL Erlenmeyer flasks. Different volumes of the NOM stock solution and 70 μL of a Cu(II) (as $Cu(NO_3)_2$) stock solution were added to obtain an initial Cu(II) concentration of 11.37 mg/L and NOM concentrations of 0–20 mg C/L. The pH of each test solution was adjusted to 6.00 ± 0.10 using either 0.1 M HNO_3 or 0.1 M NaOH. The flasks were then left to shake for 24 h at 150 rpm and 25 ± 1 °C. All experiments were performed in duplicate. After equilibration, the supernatants were filtered through 0.22 μm nylon membranes. The MWCNT samples were washed using Milli-Q water and dried at ambient temperature to yield a powder for further characterization. The Cu(II) and DOC concentrations in the filtrate were analyzed using ICP-OES (Prodigy, Leeman, USA) and the total organic carbon analyzer (TOC-V_{CPN}, Shimadzu, Japan), respectively. The adsorption amounts of Cu(II) and NOM was calculated using the differences between the initial and equilibrium concentrations.

3. Results and discussion

3.1. Characteristics of MWCNTs and NOM

3.1.1. Characteristics of MWCNTs

The elemental compositions of the three types of MWCNTs are shown in Table 2. All MWCNTs had very high organic carbon content and low N and O contents, demonstrating their high hydrophobicity. The O content increased in the order of MWCNTs-1 (2.73%) < MWCNTs-2 (5.29%) < MWCNTs-3 (7.87%) (Table 2). Moreover, higher surface O content was observed for MWCNTs-2 and MWCNTs-3 than their bulk samples in contrast to the MWCNTs-1. This indicated that the functional groups in MWCNTs-2 and MWCNTs-3 were mainly on the exterior surfaces of the MWCNTs.

Table 2
Characteristics of MWCNTs.

MWCNT	Elemental analysis (%)				XPS surface element (%)		
	N	C	H	O	C	O	N
MWCNT-1	0.05	96.85	0.37	2.73	98.2	1.8	0
MWCNT-2	0.24	93.91	0.56	5.29	87.4	12.6	0
MWCNT-3	0.18	91.26	0.69	7.87	85.5	14.5	0

3.1.2. NOM properties

The HAs (LSH, PPH, WPH, and ESH) contained more carbon than the fulvic acid and aquatic NOM (NAF, SRN, and NRN) (Table 1), which was in accordance with their greater SUVA and aromatic character (Table 3). However, FA and aquatic NOM showed higher oxygen contents than the HAs, suggesting that they contained greater concentrations of carboxyl or phenolic moieties. The polarity index ((O + N)/C) of the different NOM, calculated from the atomic ratio of (O + N) and C [23], varied greatly, from 0.38 to 0.66 (Table 1). Moreover, FA and aquatic NOM exhibited a larger polarity index than the HAs, which was consistent with their greater carboxyl group content (Table 3).

SUVA has been widely used as a surrogate measurement for the abundance of aromatic carbon in NOM [24,25]. The SUVA ranged by more than >2 fold (2.55–5.58 L/(mg C m)) (Table 3), showing considerable differences in the NOM quality. Generally, the HAs exhibited higher SUVA values than the FA and aquatic NOM (Table 3), indicating a higher aromatic carbon content in the HAs. This is consistent with the aromatic carbon content that was determined by ^{13}C NMR, as shown in Table 1.

The HAs had lower E2/E3 (absorbance ratio at 250 nm and 365 nm) values than FA and aquatic NOM, indicating higher degrees of aromaticity as confirmed by the SUVA values. E2/E3 is a bulk spectroscopic parameter that has been widely related to the degree of humification (i.e., the decomposition of organic matter) and to certain properties of NOM, such as molecular weight (MW), aromaticity and polarity [26]. As shown in Fig. 1a, HAs demonstrate higher-molecular-weight (with shorter retention time) than FA and aquatic NOM. High E2/E3 ratios indicate that NOM has a low extent of conjugation between the carbon atoms in its structure. Therefore, the E2/E3 ratio generally increases as the aromaticity and molecular weight decrease [27].

Three characteristic peaks are generally identified from the synchronous fluorescence spectra of NOM (Fig. 1b). The first peak (F1) is typically found between 250 nm and 300 nm and is ascribed to proteins and/or amino acids. The second (F2) and the third (F3) peaks appear at wavelengths of ~400 nm and ~460 nm and are attributed to fulvic-like and humic-like NOM [28–30], respectively. This was confirmed by the predominant peaks for the HAs, FA and aquatic NOM in the present study (Fig. 1b). Similar fluorescence peaks were found for soil and sediment HAs by Hur et al. [22]. The TOC-normalized fluorescence intensities (I_1–I_3) corresponding to the F1–F3 are shown in Table 3. The I_1 and I_3 both varied greatly, from 0.79 to 3.07 a.u. L/(mg C) and from 0.70 to 3.23 a.u. L/(mg C), respectively, whereas a much more narrow range of I_2 (from 0.93 to 1.81 a.u. L/(mg C)) was observed. Moreover, the HAs had lower I_1 values and higher I_3 values than FA and aquatic NOM.

3.2. NOM adsorption by MWCNTs

3.2.1. Adsorption isotherm

The adsorption of NOM onto MWCNTs was well described by the Freundlich isotherm model (R^2 > 0.81, Table 4) which has commonly been used to fit the adsorption isotherms of organic pollutants in aqueous solutions:

$$q_e = K_F C_e^n \quad (1)$$

Table 3
UV–visible, functional groups and fluorescence characteristics for the NOM samples.

	SUVA (L/(mg C m))	E2/E3	Carboxyl (meq/(g C))	Phenol (meq/(g C))	I_1 (a.u. L/(mg C))	I_2 (a.u. L/(mg C))	I_3 (a.u. L/(mg C))
LSH	4.30	2.63	7.46	2.31	0.79	1.81	3.23
PPH	5.23	2.86	8.87	2.05	0.98	1.18	2.42
WPH[a]	4.33	3.11	7.58	3.75	1.18	0.93	1.31
ESH	5.58	2.36	8.28	1.87	0.92	1.34	2.91
NAF	3.41	3.81	11.16	3.18	1.73	1.48	1.15
SRN	2.58	4.07	9.85	3.94	2.02	1.45	0.70
NRN[a]	2.55	4.50	11.93	3.25	3.07	1.69	0.92

[a] The carboxyl content and phenol group contents in WPH and NRN were determined using potentiometric automatic titration (AT-500 N, KEM, Japan) according to the method described on the IHSS website.

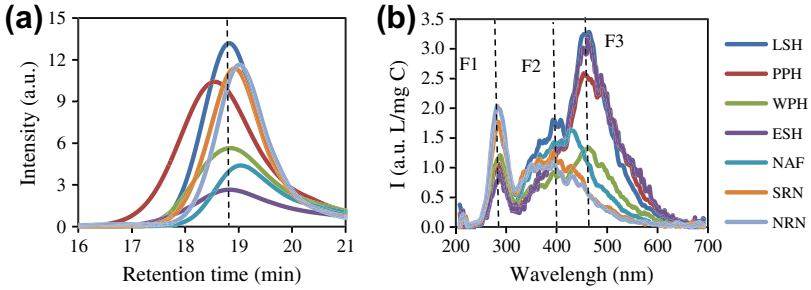

Fig. 1. (a) Size exclusion chromatograms spectra and (b) synchronous fluorescence spectra of NOM.

Table 4
Freundlich adsorption model parameters for various NOM.

NOM	MWCNTs-1			MWCNTs-2			MWCNTs-3		
	K_F	n	R^2	K_F	n	R^2	K_F	n	R^2
LSH	54.48	0.990	0.971	50.13	1.606	0.870	40.10	1.387	0.819
PPH	58.01	1.089	0.970	57.28	1.475	0.817	38.32	2.339	0.826
WPH	58.47	0.912	0.861	36.37	2.380	0.911	28.08	1.562	0.913
ESH	71.38	1.732	0.925	74.23	2.021	0.898	69.60	3.096	0.937
NAF	33.72	0.927	0.873	16.39	0.821	0.992	11.39	0.950	0.974
SRN	18.54	0.982	0.994	12.56	0.835	0.985	8.291	0.947	0.992
NRN	11.34	1.160	0.969	7.42	1.110	0.987	6.969	1.010	0.998

where q_e (mg C/g) is the sorption amount of NOM, C_e (mg C/L) is the equilibrium NOM concentration, and K_F ($L^n(mg\ C)^{1-n}/g$) and n (dimensionless) represent a Freundlich constant and Freundlich exponent, respectively.

As shown in Table 4, the K_F values changed greatly (>6 fold for MWCNTs-1, >10 fold for MWCNTs-2, and >9 fold MWCNTs-3) for the different types of NOM. Generally, the less-soluble and higher-molecular-weight HAs had higher K_F values than FA and aquatic NOM. This is in agreement with what was previously found by Hyung and Kim [15], and may suggest that micropore filling is not a major sorption mechanism for NOM [31]. Due to the larger molecular size of NOM, the steric hindrance between NOM and MWCNTs makes it difficult for the NOM molecules to penetrate into the micropores of MWCNTs.

However, the NOM adsorption onto MWCNTs was also closely related to the functional groups that were on the surfaces of the MWCNTs. The MWCNTs-1 with the lowest O content had the highest K_F values, followed by MWCNTs-2 and MWCNTs-3. NMR and elemental composition data (Table 1) showed that the NOM were rich in O-containing groups. Although these moieties in NOM can interact with polar functional groups (OH and COOH) on the graphene surfaces of the MWCNTs via hydrogen bonding [32], the hydrogen bonding would most likely be low due to the limited O content on the MWCNT surfaces (Table 2). The higher K_F values for the MWCNTs-1 indicated that the sorption of NOM by individual MWCNTs was dependent on the hydrophobicity of the MWCNTs. The functional groups OH and COOH on the surfaces of MWCNTs-2 and MWCNTs-3 altered the polarities of the MWCNTs and decreased the adsorption of the high-molecular-weight and nonpolar NOM [9]. The creation of polar regions on the surfaces of the MWCNTs [33] or the formation of water clusters around the O-containing groups [34] were previously shown to decrease the adsorption capacities of hydrophobic chemicals. Additionally, an increase in the oxygen content of the MWCNTs was previously shown to decrease the adsorption of naphthalene, diuron, and dichlobenil [33,35]. The present results revealed that hydrophobic interactions may be one of the mechanisms that affect NOM adsorption onto MWCNTs.

3.2.2. Relationship between NOM adsorption and its properties

As shown in Table 4, the adsorptive interactions between NOM and MWCNTs were strongly dependent on the type of NOM. Among the various functional groups in NOM that were determined by ^{13}C NMR (Table 1), the aromatic carbon content exhibited the strongest linear relationship with K_F ($R^2 > 0.65$, $p < 0.05$, Fig. 2a). Hyung and Kim [15] also previously reported good correlations between aromaticity and the adsorption capacity of NOM by MWCNTs. Similarly, K_F also showed a positive linear relationship with SUVA ($R^2 > 0.84$, $p < 0.01$, Fig. 2b). In contrast, a negative relationship between E2/E3 and the K_F values was observed ($R^2 > 0.85$, $p < 0.01$, Fig. 2c). It is well known that E2/E3 increases as the NOM molecular weight and aromaticity decrease [26,27].

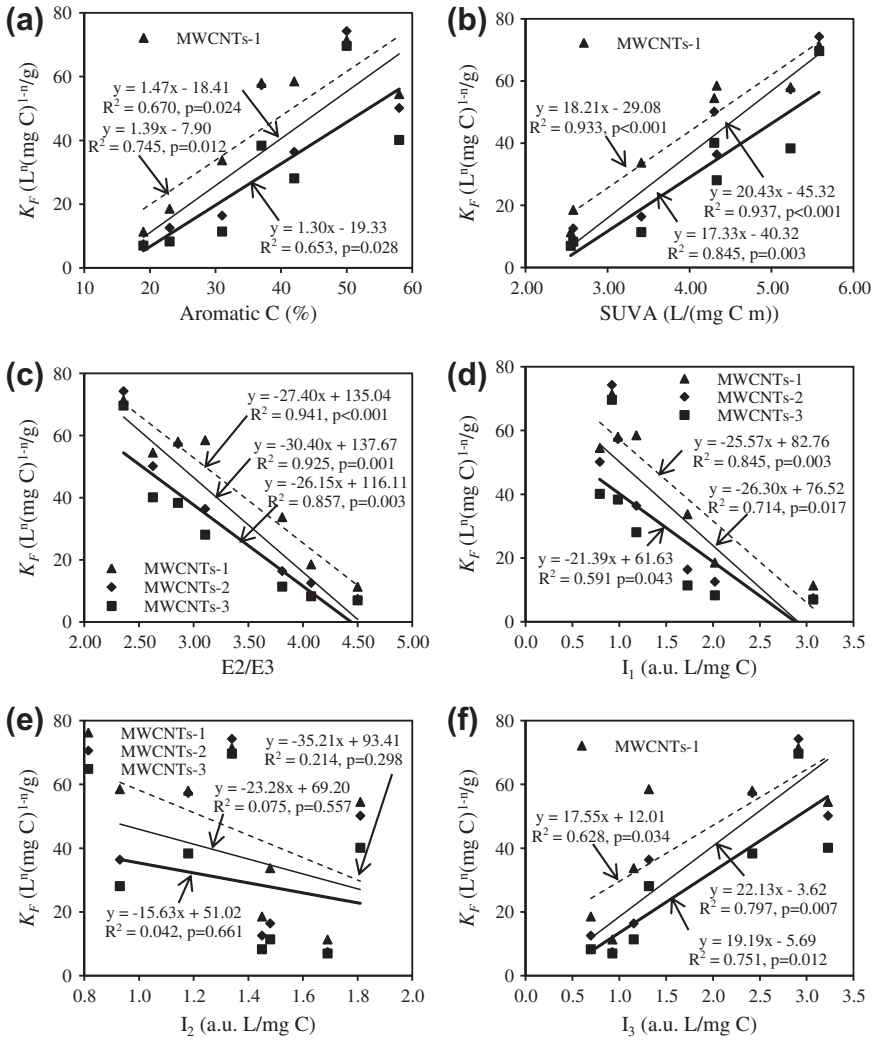

Fig. 2. Relationship between the aromatic group contents of the NOM and the NOM adsorption constants (K_F). Dashed line – MWCNTs-1, solid line – MWCNTs-2, and bold line – MWCNTs-3.

The preferential adsorption of the higher-molecular-weight fraction of NOM was also observed by Hyung and Kim [15]. The results from this study suggest that the aromatic moieties in NOM play important roles in NOM adsorption by MWCNTs.

K_F had a strong negative linear correlation with I_1 ($R^2 > 0.59$, $p < 0.05$, Fig. 2d) and a significant positive linear relationship with I_3 ($R^2 > 0.62$, $p < 0.05$, Fig. 2f), while no significant relationship was observed between K_F and I_2 ($p > 0.29$, Fig. 2e). Fluorescence is increasingly used to characterize NOM in water, sediments and soils. It is well known that the F1 peak is a good indicator of the presence of proteins and/or amino acids [22,25], F2 is attributed to the FA components with the lower degrees of aromaticity, and F3 is associated with the polycondensation of phenolic aromatic units, such as HAs [28–30]. Therefore, NOM adsorption by MWCNTs showed a strong negative correlation with the concentrations of proteins and/or amino acids and demonstrated a positive correlation with the extent of the polycondensation of phenolic aromatic units in NOM. This may indicate that the molecular weight or the hydrophobicity of NOM influences its adsorption onto MWCNTs. Hyung and Kim [15] also observed the preferential adsorption of high-molecular-weight NOM onto MWCNTs.

The present results suggest that the π–π interactions that take place between the benzene rings of NOM and the graphene sheets of MWCNTs are an important mechanism governing the NOM sorption [36]. As reported by previous studies [32,37], organic molecules that contain π electrons, such as C=C double bonds or benzene rings, can form π–π bonds with CNTs. In addition, the hydrophobic interaction mechanism may act simultaneously considering the polarity of MWCNTs and the molecular weight of NOM. Yang and Xing [17] also showed that the apparent interaction mechanisms between FA and CNT surfaces included hydrophobic and π–π interactions. The present results also imply that the aromatic content and hydrophobicity of NOM could be useful for evaluating the level of NOM adsorption onto MWCNTs.

3.3. Effect of NOM on Cu(II) adsorption by MWCNTs

3.3.1. Cu(II) adsorption at different NOM concentrations

In the absence of NOM, the adsorption amount of Cu(II) by the MWCNTs increased in the order of MWCNTs-1 (3.580 mg/g) < MWCNTs-2 (7.286 mg/g) < MWCNTs-3 (8.226 mg/g) (Fig. 3). In other words, the Cu(II) adsorption increased as the O content in the MWCNTs increased (Table 2), suggesting that the O-containing groups on the surfaces of the MWCNTs favored Cu(II) adsorption by complexing with Cu(II). Chen et al. [6] also found that oxygen-containing groups, mainly carboxylic groups, significantly increased the adsorption of lead through the formation of outer-sphere and inner-sphere complexes. The significant increase in

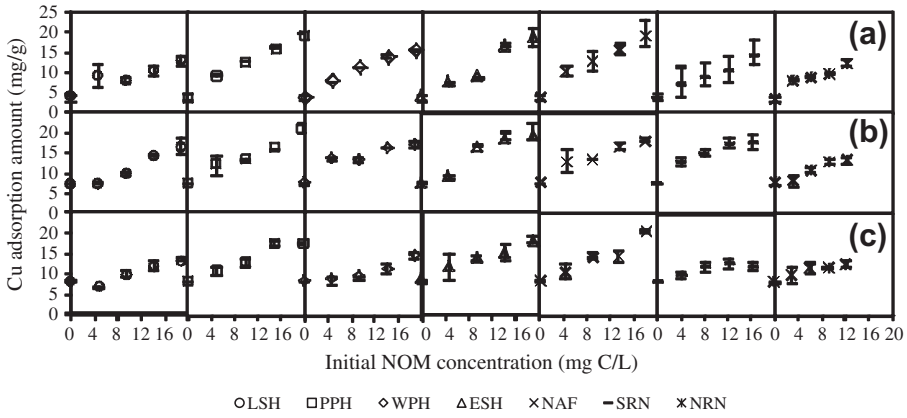

Fig. 3. Adsorption of Cu(II) by MWCNTs at different initial NOM concentrations. (a) MWCNTs-1, (b) MWCNTs-2, and (c) MWCNTs-3.

Cu(II) adsorption also confirmed the hydrophilic and cation-exchange properties for MWCNTs-2 and MWCNTs-3 [4].

The amount of Cu(II) adsorption increased with increasing initial NOM concentrations, and similar results were observed for various types of NOM and MWCNTs (Fig. 3). This indicated that the addition of NOM favored the Cu(II) adsorption by MWCNTs, which is different from the behavior observed for aromatic compounds. Wang et al. [31] found that HA competed with phenanthrene and 1-naphthol and thus reduced their sorption by MWCNTs. Here, however, NOM could adsorb onto the surfaces of the MWCNTs and then promote the adsorption of Cu(II) due to its binding with Cu(II). A positive effect of HA/FA on Cu(II) adsorption was also previously observed at pH < 7.5 by Sheng et al. [7]. However, Yang et al. [38] found that Pb(II) adsorption onto polyacrylamide-grafted MWCNTs increases with increasing HA concentration at C_{HA} < 7.5 mg/L or C_{HA} > 12.5 and decreases with increasing HA concentration at 7.5 < C_{HA} < 12.5 mg/L at pH 5. The different adsorption behavior of Pb(II) with rising HA concentration at 7.5 < C_{HA} < 12.5 mg/L and C_{HA} > 12.5 mg/L could be ascribed to the much more polar surface of polyacrylamide-grafted MWCNTs. Zhao et al. [39] also found the strong surface complexation and high surface site density of grapheme oxide nanosheets resulted in the decreased adsorption of Cd(II) and Co(II) in the presence of HA. This reveals that the surface properties of adsorbents influence the effect of HA on the adsorption of metals.

The chemical states and the binding energies of each element in the samples were determined by XPS (Fig. 4). The main peaks at binding energies of 284 eV and 533 eV corresponded to the C 1s and O 1s (Fig. 4a), respectively. The high-resolution XPS spectra of the MWCNTs, MWCNTs–Cu(II), MWCNTs–NOM, and MWCNTs–NOM–Cu(II) samples at C 1s (b), O 1s (c), and Cu 2p (d) core levels are also shown in Fig. 4. Three high-resolution XPS C 1s peaks positioned at 284.8, 285.6, and 288.8 eV were assigned to bridging C—C (charge referenced to 284.80 eV), C—O and O—C=O groups [40], respectively. The relative intensities of the last two carbon groups slightly increased in the MWCNTs–NOM sample (Fig. 4b), both of which were attributed to the adsorption of NOM onto the surfaces of the MWCNTs. In addition, significant increases in the intensity of O 1s were observed in the MWCNTs–NOM sample (Fig. 4c), which could be fitted to two line shapes with binding energies at 533.3 eV (C—O) and 531.8 eV (O—C=O), respectively [41]. These results indicated that the functional groups of NOM were introduced to the MWCNTs. A shift of approximately 0.3 eV of the two O 1s peaks was observed in the MWCNTs–NOM–Cu(II) system, most likely as a result of the complexation between Cu(II) and NOM on the surfaces of the MWCNTs. Two peaks of Cu $2p_{3/2}$ and Cu $2p_{1/2}$ were observed at 934.2 and 954.2 eV, respectively, in the MWCNTs–Cu(II) and MWCNTs–NOM–Cu(II) samples (Fig. 4d) [42,43], which confirmed the loading of the Cu(II) in the MWCNTs. Furthermore, compared with the MWCNTs–Cu(II) sample, the dramatic increase of the intensity of Cu 2p in the MWCNTs–NOM–Cu(II) sample indicated the facilitation effect of NOM on the adsorption of Cu(II) by MWCNTs.

The increased Cu(II) adsorption with rising NOM could be attributed to the complexation of Cu(II) with adsorbed NOM, which was verified by FTIR analysis (Fig. 4e). All spectra had a broad band approximately 3400 cm^{-1}, which was generally attributed to the stretching vibration of the O—H groups [13,44]. The absorption at 1632 cm^{-1} in the MWCNTs indicated the existence of an aromatic C=C structures in the raw MWCNTs [45]. Peaks were observed at 1720, 1628, 1400, 1212, 1082 and 1050 cm^{-1} in the NOM alone. The dramatic decrease in the intensity of the peak at 1628 cm^{-1} in the MWCNTs–NOM sample indicated the presence of strong interactions between the aromatic C=C of the NOM and the MWCNTs. In addition, interactions between the COOH and phenolic OH groups of the NOM and the MWCNT surfaces may have occurred due to the disappearance of the peaks at 1720 and 1212 cm^{-1} [44,46]. An obvious decrease and shift of the peak at 1566 cm^{-1} was observed after the addition of Cu(II), which could have resulted from the binding effect of Cu(II) with the COO^- groups [46].

3.3.2. The increased degree of Cu(II) adsorption by different types of NOM

Based on the FTIR spectra (Fig. 4e), it was deduced that the binding of adsorbed NOM with Cu(II) promoted the uptake of Cu(II) by MWCNTs. To better understand the relationship between NOM properties and their effects on Cu(II) adsorption, a linear regression between adsorbed Cu(II) and adsorbed NOM was performed. A close linear relationship (R^2 > 0.73, p < 0.05, Table 5) was observed between the adsorbed Cu(II) and adsorbed NOM, and the slope of the linear equation (k, mg/(g C)) was used to quantify the increased degree of Cu(II) adsorption by the different types of NOM.

The calculated k values (Table 5) varied depending on the type of NOM and MWCNTs, and they ranged from 114.4 mg/(g C) to 218 mg/(g C) for MWCNTs-1, from 102.0 mg/(g C) to 185.0 mg/(g C) for MWCNTs-2, and from 59.6 mg/(g C) to 184.5 mg/(g C) for MWCNTs-3. FA and aquatic NOM generally had relatively larger k values than HA, suggesting high Cu(II) binding affinities of low-molecular-weight NOM as demonstrated by Marschner and Bredow [47]. This was ascribed to the increased numbers of functional groups (e.g., OH and/or COOH) in FA and aquatic NOM that could complex with Cu(II). Furthermore, the greater k values of FA and aquatic NOM could also be explained by the higher polarities of those types of NOM, as indicated by their (N + O)/C ratios (Table 1) [23].

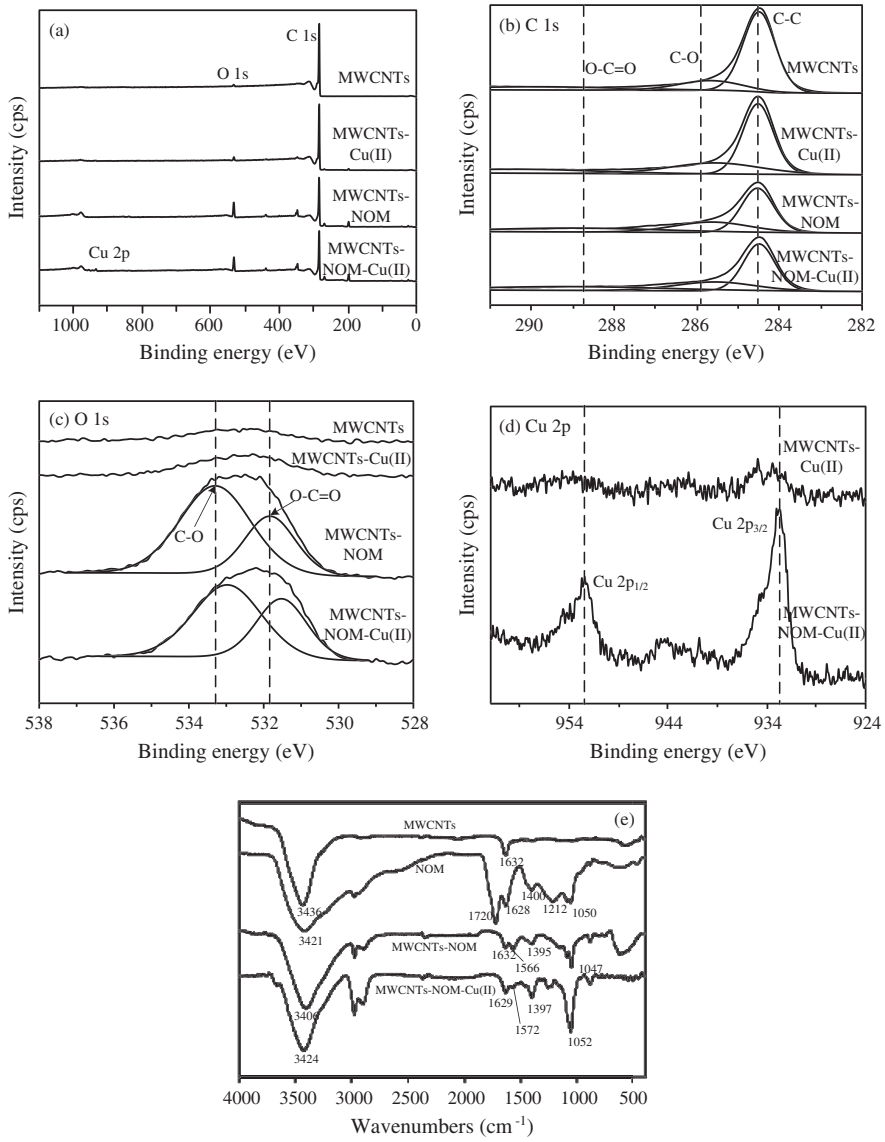

Fig. 4. (a) Representative XPS spectra of survey, (b) C 1s, (c) O 1s and (d) Cu 2p spectra of MWCNTs, MWCNTs–Cu(II), MWCNTs–NOM, and MWCNTs–NOM–Cu(II) and (e) FTIR spectra of MWCNTs, NOM, MWCNTs–NOM, and MWCNTs–NOM–Cu(II) (MWCNTs-1 and SRN, TOC = 14.75 mg/L, Cu = 11.37 mg/L).

Table 5
Binding affinities (k, mg/g C) of Cu(II) by adsorbed NOM.

NOM	MWCNTs-1		MWCNTs-2		MWCNTs-3	
	k (mg/g C)	R^2	k (mg/g C)	R^2	k (mg/g C)	R^2
LSH	114.4	0.810	102.0	0.903	59.6	0.784
PPH	179.6	0.977	140.8	0.960	113.0	0.946
WPH	146.6	0.962	127.8	0.734	61.3	0.825
ESH	171.9	0.954	163.1	0.924	116.0	0.964
NAF	218.4	0.951	185.0	0.904	184.5	0.924
SRN	170.1	0.963	170.0	0.881	106.2	0.778
NRN	199.2	0.818	167.0	0.974	129.4	0.919

Moreover, the NOM that was bound to various MWCNTs demonstrated different k values in the order of MWCNTs-1 > MWCNTs-2 > MWCNTs-3. This order was the same as that of the NOM adsorption (K_F, Table 4). This was mainly related to the properties of the MWCNTs. The MWCNTs were able to compete with the NOM for complexing with Cu(II). Moreover, the MWCNTs with a higher content of oxygen had greater abilities to compete, as demonstrated by their higher Cu(II) adsorption amounts in the absence of NOM. Hydrogen bonding may have occurred between the functional groups of NOM and those on the surfaces of MWCNTs-2 and MWCNTs-3, although it was not the main mechanism of NOM adsorption. This hydrogen bonding between the NOM and the MWCNTs could hinder Cu(II) binding by NOM and consequently decrease the Cu(II) binding affinity (k) by the adsorbed NOM. Additionally, due to the surface shielding of MWCNTs by NOM, the MWCNTs that are intermediately situated inside the NOM might block the functional groups by steric stabilization [13]. This blocking effect would be more evident for functionalized MWCNTs with higher Cu(II) adsorption capacities and likely explains the lower calculated k values for MWCNTs-2 and MWCNTs-3.

3.3.3. Relationship between NOM properties and Cu(II) adsorption

The k values were significantly and positively correlated with the carboxyl carbon content ($R^2 > 0.74$, $p < 0.05$, Fig. 5a) and carboxyl group content ($R^2 > 0.62$, $p < 0.05$, Fig. 5b) of the NOM. This suggested that the functional group COOH plays an important role in binding Cu(II) by the adsorbed NOM. Rey-Castro et al. [18] found that the binding of Cu(II) with NOM was shared equally between the carboxylic and phenolic sites of NOM. However, no evident relationship was found between the k values and the phenol group

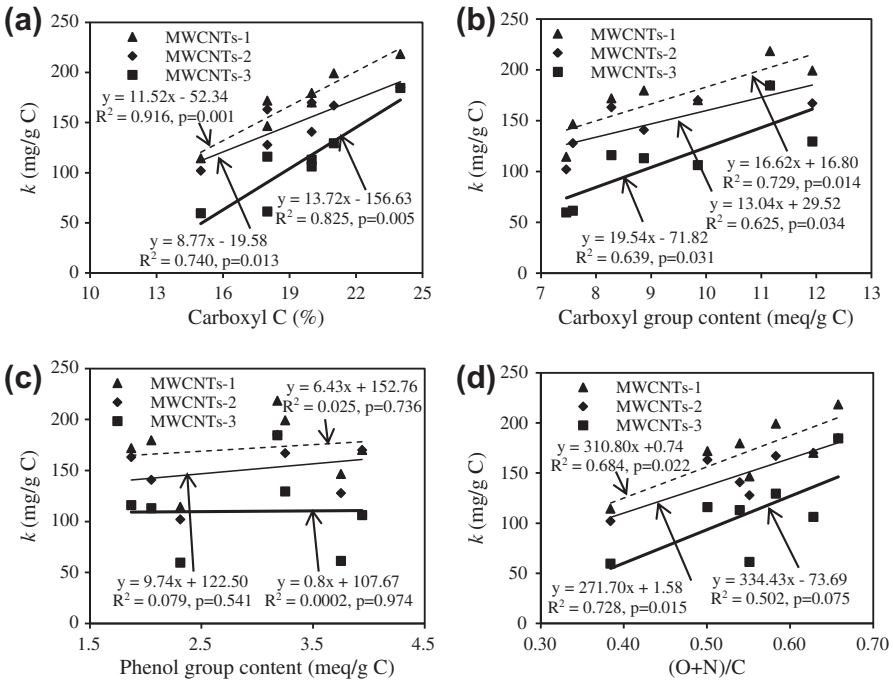

Fig. 5. Relationship between Cu(II) binding affinity to adsorbed NOM (k) and NOM properties. Dashed line – MWCNTs-1, solid line – MWCNTs-2, and bold line – MWCNTs-3.

content of the NOM ($p > 0.54$, Fig. 5c). This could be ascribed to the lower phenolic group content in the NOM (Table 3) and the lower pH (6) that was used in the present study compared to the pH of 7 that was used by Rey-Castro et al. [18]. At pH 6, carboxylic groups are deprotonated, while phenolic groups are protonated. Therefore, Cu(II) is preferentially bound to carboxylic sites at pH 6. In addition, in agreement with Baken et al. [19], no significant correlation was observed between the k values and SUVA or aromatic carbon content (data not shown). This suggested that the Cu(II) binding with NOM was independent of aromatic moieties.

As demonstrated in Fig. 5d, the k values had significant ($p < 0.05$) positive linear correlations with the polarity index of NOM, with an R^2 of 0.684 for MWCNTs-1 and an R^2 of 0.728 for MWCNTs-2. This also indicated that the binding between Cu(II) and adsorbed NOM was related to the polar functional groups as confirmed by Fig. 5a and b. As reported by Wang and Xing [48],

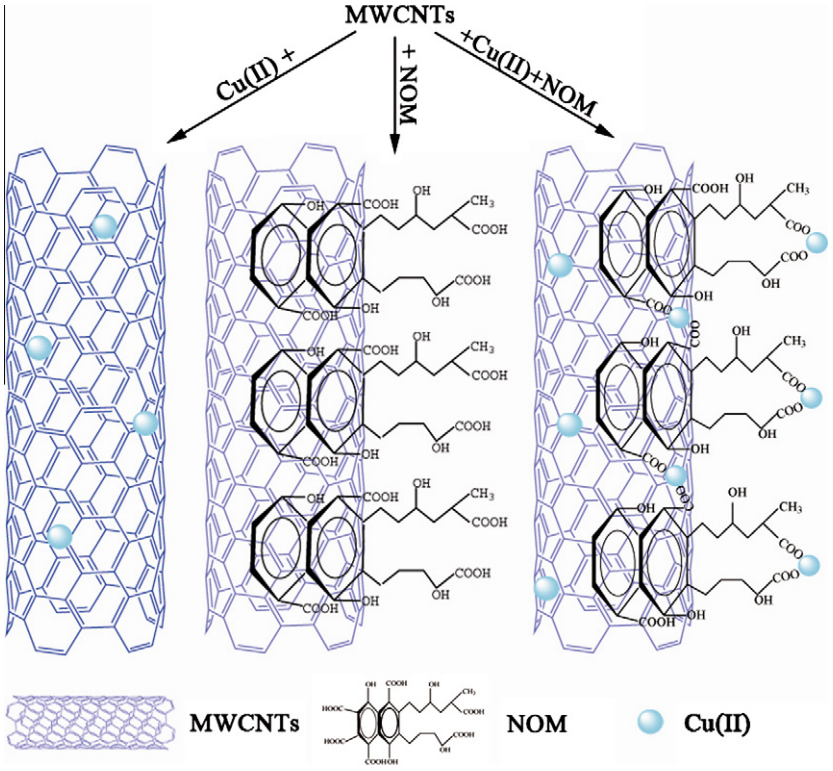

Fig. 6. Schematic diagram of interactions between Cu(II), MWCNTs, and NOM.

the present study suggests that O-containing hydrophilic functional groups in NOM, especially carboxylic group, serve as ligands to form complexes with Cu(II). However, a low positive linear correlation between k values and the polarity index of NOM was observed for MWCNTs-3 ($R^2 = 0.502$, $p = 0.075$). This could be ascribed to the higher binding abilities between Cu(II) and MWCNTs or the hydrogen binding between the NOM and the MWCNTs due to the higher oxygen content in MWCNTs-3.

The interactions between Cu(II), MWCNTs, and NOM were shown in Fig. 6. NOM was adsorbed by MWCNTs mainly through π–π and hydrophobic interactions, and thus aromaticity was a key factor for NOM sorption onto MWCNTs. In the presence of NOM, the Cu (II) adsorption was promoted significantly by NOM via complexing of Cu (II) with carboxylic groups in the MWCNTs–adsorbed NOM molecular. So the increased degree of Cu(II) adsorption was correlated with the carboxyl group contents of the NOM.

3.4. Environmental significance

Our results highlight that the molecular components of NOM or the NOM properties are responsible for influencing NOM adsorption and its effects on heavy metal adsorption by MWCNTs. NOM is ubiquitous in the natural environment, but it demonstrates different characteristics from different sources; nonetheless, it is easily adsorbed onto MWCNTs and changes the adsorption behavior of metals significantly. Aromaticity is a key factor for NOM sorption onto MWCNTs, while its O-containing hydrophilic functional groups play critical roles in its effect on Cu(II) adsorption. Therefore, the interaction between stabilized MWNTs in NOM and other coexisting toxic compounds should be seriously considered when the environmental risks of carbon nanomaterials are evaluated.

4. Conclusions

The NOM adsorption by MWCNTs was well described by the Freundlich isotherm model. The Freundlich constant K_F for various NOM samples was proportional to the aromatic carbon content and SUVA and had a negative linear correlation with E2/E3. The three characteristic peaks (F1: 250–300 nm, F2: ∼400 nm, and F3: ∼460 nm) were identified from the synchronous fluorescence spectra of NOM. They were assigned to proteins and/or amino acids, fulvic-like NOM, and humic-like NOM, respectively. The K_F had a strong negative linear correlation with the TOC-normalized fluorescence intensity of F1 (I_1) and a significant positive linear relationship with the TOC-normalized fluorescence intensity of F3 (I_3). The results indicated that π–π and hydrophobic interactions were predominant NOM adsorption mechanisms by MWCNTs. The Cu(II) adsorption by the MWCNTs increased with increasing NOM concentrations due to the complexing of Cu(II) with adsorbed NOM. The increased degree of Cu(II) adsorption was positively correlated with the carboxyl carbon content, carboxyl group content and the polarity index ((O + N)/C) of the NOM, suggesting that O-containing hydrophilic functional groups, especially carboxyl groups, in NOM play a critical role in complexing with Cu(II). Moreover, the polarities of the MWCNTs also influenced the Cu(II) binding affinities with the adsorbed NOM.

Acknowledgement

This research was funded by the National Natural Science Foundation of China (Grant No. 51079002).

References

[1] R.E. Service, Superstrong nanotubes show they are smart, too, Science 281 (1998) 893–894.
[2] S.J. Klaine, P.J.J. Alvarez, G.E. Batley, T.F. Fernandes, R.D. Handy, D.Y. Lyon, S. Mahendra, M.J. Mclaughlin, J.R. Lead, Nanomaterials in the environment: behavior, fate, bioavailability, and effects, Environ. Toxicol. Chem. 27 (2008) 1825–1851.
[3] J.X. Li, S.Y. Chen, G.D. Sheng, J. Hu, X.L. Tan, X.K. Wang, Effect of surfactants on Pb(II) adsorption from aqueous solutions using oxidized multiwall carbon nanotubes, Chem. Eng. J. 166 (2011) 551–558.
[4] M.I. Kandah, J.L. Meunier, Removal of nickel ions from water by multi-walled carbon nanotubes, J. Hazard. Mater. 146 (2007) 283–288.
[5] M. Tuzen, K.O. Saygi, M. Soylak, Solid phase extraction of heavy metal ions in environmental samples on multiwalled carbon nanotubes, J. Hazard. Mater. 152 (2008) 632–639.
[6] C.L. Chen, J. Hu, D.D. Shao, J.X. Li, X.K. Wang, Adsorption behavior of multiwall carbon nanotube/iron oxide magnetic composites for Ni(II) and Sr(II), J. Hazard. Mater. 164 (2009) 923–928.
[7] G.D. Sheng, J.X. Li, D.D. Shao, J. Hu, C.L. Chen, Y.X. Chen, X.K. Wang, Adsorption of copper(II) on multiwalled carbon nanotubes in the absence and presence of humic or fulvic acids, J. Hazard. Mater. 178 (2010) 333–340.
[8] M.A. Tofighy, T. Mohammadi, Adsorption of divalent heavy metal ions from water using carbon nanotube sheets, J. Hazard. Mater. 185 (2011) 140–147.
[9] K. Yang, B.S. Xing, Adsorption of organic compounds by carbon nanomaterials in aqueous phase: Polanyi theory and its application, Chem. Rev. 110 (2010) 5989–6008.
[10] M.N. Moore, Do nanoparticles present ecotoxicological risks for the health of the aquatic environment?, Environ Int. 32 (2006) 967–976.
[11] B. Nowack, T.D. Bucheli, Occurrence, behavior and effects of nanoparticles in the environment, Environ. Pollut. 150 (2007) 5–22.
[12] G.S. Simatea, S.E. Iyukea, S. Ndlovua, M. Heydenrychb, L.F. Walubitac, Human health effects of residual carbon nanotubes and traditional water treatment chemicals in drinking water, Environ. Int. 39 (2012) 38–49.
[13] K.T. Kim, A.J. Edgington, S.J. Klaine, J.W. Chao, S.D. Kim, Influence of multiwalled carbon nanotubes dispersed in natural organic matter on speciation and bioavailability of copper, Environ. Sci. Technol. 43 (2009) 8979–8984.
[14] E.M. Thurman, Organic Geochemistry of Natural Waters, United States Geological Survey, Denver, Colorado, USA, 1985.
[15] H. Hyung, J.H. Kim, Natural organic matter (NOM) adsorption to multi-walled carbon nanotubes: effect of NOM characteristics and water quality parameters, Environ. Sci. Technol. 42 (2008) 4416–4421.
[16] S.J. Zhang, T. Shao, T. Karanfil, The effects of dissolved natural organic matter on the adsorption of synthetic organic chemicals by activated carbons and carbon nanotubes, Water Res. 45 (2011) 1378–1386.
[17] K. Yang, B.S. Xing, Adsorption of fulvic acid by carbon nanotubes from water, Environ. Pollut. 157 (2009) 1095–1100.
[18] C. Rey-Castro, S. Mongin, C. Huidobro, C. David, J. Salvador, J.L. Garcés, J. Galceran, F. Mas, J. Puy, Effective affinity distribution for the binding of metal ions to a generic fulvic acid in natural waters, Environ. Sci. Technol. 43 (2009) 7184–7191.
[19] S. Baken, F. Degryse, L. Verheyen, R. Merckx, E. Smolders, Metal complexation properties of freshwater dissolved organic matter are explained by its aromaticity and by anthropogenic ligands, Environ. Sci. Technol. 45 (2011) 2584–2590.
[20] P.A. Neale, A. Antony, W. Gemjak, G. Leslie, B.I. Escher, Natural versus wastewater derived dissolved organic carbon: implications for the environmental fate of organic micropollutants, Water Res. 45 (2011) 4227–4237.
[21] A. Deonarine, B.L.T. Lau, G.R. Aiken, J.N. Ryan, H. Hsu-Kim, Effects of humic substances on precipitation and aggregation of zinc sulfide nanoparticles, Environ. Sci. Technol. 45 (2011) 3217–3223.
[22] J. Hur, B.M. Lee, H.S. Shin, Comparison of the structural, spectroscopic and phenanthrene binding characteristics of humic acids from soils and lake sediments, Org. Geochem. 40 (2009) 1091–1099.
[23] S. Kang, B. Xing, Humic acid fractionation upon sequential adsorption onto goethite, Langmuir 24 (2008) 2525–2531.
[24] W.L. Sun, T.T. Liu, F. Cui, J.R. Ni, Fluorescence evolution of leachates during treatment processes from two contrasting landfills, Environ. Technol. 29 (2008) 1119–1125.
[25] J. Hur, B.M. Lee, H.S. Shin, Microbial degradation of dissolved organic matter (DOM) and its influence on phenanthrene–DOM interactions, Chemosphere 85 (2011) 1360–1367.
[26] J. Peuravuori, K. Pihlaja, Molecular size distribution and spectroscopic properties of aquatic humic substances, Anal. Chim. Acta 337 (1997) 133–149.
[27] C.S. Uyguner, M. Bekbolet, Implementation of spectroscopic parameters for practical monitoring of natural organic matter, Desalination 176 (2005) 47–55.
[28] T.M. Miano, N. Senesi, Synchronous excitation fluorescence spectroscopy applied to soil humic substances chemistry, Sci. Total Environ. 117 (1992) 41–51.
[29] X.Q. Lu, R. Jaffe, Interaction between Hg(II) and natural dissolved organic matter: a fluorescence spectroscopy based study, Water Res. 35 (2001) 1793–1803.
[30] X.Q. Lu, N. Maie, J.V. Hanna, D.L. Childers, R. Jaffé, Molecular characterization of dissolved organic matter in freshwater wetlands of the Florida Everglades, Water Res. 37 (2003) 2599–2606.
[31] X.L. Wang, S. Tao, B.S. Xing, Sorption and competition of aromatic compounds and humic acid on multiwalled carbon nanotubes, Environ. Sci. Technol. 43 (2009) 6214–6219.

[32] D.H. Lin, B.S. Xing, Adsorption of phenolic compounds by carbon nanotubes: role of aromaticity and substitution of hydroxyl groups, Environ. Sci. Technol. 42 (2008) 7254–7259.
[33] H.H. Cho, B.A. Smith, J.D. Wnuk, D.H. Fairbrother, W.P. Ball, Influence of surface oxides on the adsorption of naphthalene onto multiwalled carbon nanotubes, Environ. Sci. Technol. 42 (2008) 2899–2905.
[34] S.J. Zhang, T. Shao, S.S.K. Bekaroglu, T. Karanfil, The impacts of aggregation and surface chemistry of carbon nanotubes on the adsorption of synthetic organic compounds, Environ. Sci. Technol. 43 (2009) 5719–5725.
[35] G.C. Chen, X.Q. Shan, Z.G. Pei, H.H. Wang, L.R. Zheng, J. Zhang, Y.N. Xie, Adsorption of diuron and dichlobenil on multiwalled carbon nanotubes as affected by lead, J. Hazard. Mater. 188 (2011) 156–163.
[36] J. Zhang, J.K. Lee, Y. Wu, R.W. Murray, Photoluminescene and electronic interaction of anthracene derivatives adsorbed on sidewalls of single-walled carbon nanotubes, Nano Lett. 3 (2003) 403–407.
[37] W. Chen, L. Duan, L. Wang, D.Q. Zhu, Adsorption of hydroxyl and amino-substituted aromatics to carbon nanotubes, Environ. Sci. Technol. 42 (2008) 6862–6868.
[38] S.B. Yang, J. Hu, C.L. Chen, D.D. Shao, X.K. Wang, Mutual effects of Pb(II) and humic acid adsorption on multiwalled carbon nanotubes/polyacrylamide composites from aqueous solutions, Environ. Sci. Technol. 45 (2011) 3621–3627.
[39] G.X. Zhao, J.X. Li, X.M. Ren, C.L. Chen, X.K. Wang, Few-layered graphene oxide nanosheets as superior sorbents for heavy metal ion pollution management, Environ. Sci. Technol. 45 (2011) 10454–10462.
[40] X.L. Tan, M. Fang, J.X. Li, Y. Lu, X.K. Wang, Adsorption of Eu(III) onto TiO_2: effect of pH, concentration, ionic strength and soil fulvic acid, J. Hazard. Mater. 168 (2009) 458–465.
[41] X.N. Li, H.M. Zhao, X. Quan, S. Chen, Y.B. Zhang, H.T. Yu, Adsorption of ionizable organic contaminants on multi-walled carbon nanotubes with different oxygen contents, J. Hazard. Mater. 186 (2011) 407–415.
[42] A. Naveau, F. Monteil-Rivera, E. Guillon, J. Dumonceau, XPS and XAS studies of copper(II) sorbed onto a synthetic pyrite surface, J. Colloid Interf. Sci. 303 (2006) 25–31.
[43] M. Salavati-Niasari, M. Bazarganipour, Synthesis, characterization and catalytic oxidation properties of multi-wall carbon nanotubes with a covalently attached copper(II) salen complex, Appl. Surf. Sci. 255 (2009) 7610–7617.
[44] S.W. Huang, P.N. Chiang, J.C. Liu, J.T. Hung, W.H. Kuan, Y.M. Tzou, S.L. Wang, J.H. Huang, C.C. Chen, M.K. Wang, R.H. Loeppert, Chromate reduction on humic acid derived from a peat soil – exploration of the activated sites on HAs for chromate removal, Chemosphere 87 (2012) 587–594.
[45] H.B. Fu, X. Quan, Complexes of fulvic acid on the surface of hematite, goethite, and akaganeite: FTIR observation, Chemosphere 63 (2006) 403–410.
[46] K. Yang, D.H. Lin, B.S. Xing, Interactions of humic acid with nanosized inorganic oxides, Langmuir 25 (2009) 3571–3576.
[47] B. Marschner, A. Bredow, Temperature effects on release and ecologically relevant properties of dissolved organic carbon in sterilised and biologically active soil samples, Soil Biol. Biochem. 34 (2002) 459–466.
[48] K.J. Wang, B.S. Xing, Structural and sorption characteristics of adsorbed humic acid on clay minerals, J. Environ. Qual. 34 (2005) 342–349.